

LETTERS

The purpose of this Letters section is to provide rapid dissemination of important new results in the fields regularly covered by *Physics of Fluids*. Results of extended research should not be presented as a series of letters in place of comprehensive articles. Letters cannot exceed four printed pages in length, including space allowed for title, figures, tables, references and an abstract limited to about 100 words. There is a three-month time limit, from date of receipt to acceptance, for processing Letter manuscripts. Authors must also submit a brief statement justifying rapid publication in the Letters section.

The atomic detail of a wetting/de-wetting flow

Jonathan B. Freund

*Theoretical and Applied Mechanics, University of Illinois at Urbana-Champaign,
Urbana, Illinois 61801-2983*

(Received 1 October 2002; accepted 4 February 2003; published 2 April 2003)

Atomistic simulation is used to study flow in the vicinity of the advancing (wetting) and receding (de-wetting) solid–liquid–vapor contact lines of a two-dimensional (in the mean) liquid drop in thermodynamic equilibrium with its own vapor and moving steadily on an atomically smooth solid surface under the influence of an applied body force. Wetting and de-wetting are found to be asymmetric, counter to some predictions based on linear theory. There is a rolling flow of the liquid in the drop and a dividing streamline extends from the wetting common line into the displaced vapor as observed macroscopically. At the de-wetting common line there is substantial evaporation, which alters the flow field behind the drop. Evaporation is also observed above the advancing contact line, but there is a net mass flux into the drop right at the contact line. There is evidence of slip flow just in advance of the wetting contact line, but not at the de-wetting line. Results are discussed in the context of phase-field models. © 2003 American Institute of Physics. [DOI: 10.1063/1.1565112]

It is well understood that standard hydrodynamic models with a no-slip wall boundary condition and zero mass flux phase boundaries are unphysical where a liquid–vapor phase boundary moves across a solid surface. The interface moves, but the fluid on the solid cannot if the no-slip condition is enforced. This leads to a flow which is permitted kinematically but has a stress singularity for standard constitutive relationships.¹ To avoid this, slip boundary conditions^{2–4} and a mass fluxes through the interface^{5–7} have both been proposed. Both can relieve the stress singularity. Evaporation and condensation mass fluxes have been modeled with phase-field equations that couple the flow to a chemical potential.^{5–7} Unfortunately, both the slip and phase-field models are for atomic-scale regions that are unobservable in experiments.

In this Letter we make new observations of the flow in the vicinity of the wetting and de-wetting triple lines of a small liquid roll (a drop that is two-dimensional in the mean) moving on an atomically smooth solid substrate in equilibrium with its own vapor (Fig. 1). This flow is studied by simulating the trajectories of 6016 atoms, of which 1760 are in a face-centered cubic solid phase with an exposed (100) surface and 4256 are in fluid phases, either liquid or vapor. The atoms interact via the Lennard-Jones pair potential,

$$u(r) = 4\epsilon_{ab} \left[\left(\frac{\sigma}{r} \right)^{12} - \left(\frac{\sigma}{r} \right)^6 \right].$$

The size parameter σ is the same for all interactions. The stiff solid wall is modeled by setting $\epsilon_{ss} = 100\epsilon_{ff} = 100\epsilon$. The fluid–solid interaction energy is $\epsilon_{fs} = 0.562\epsilon$, which

gives an anticipated contact angle of $\theta \approx \cos^{-1}(2\epsilon_{sf}/\epsilon - 1) = 83^\circ$.⁸ This formula neglects interactions with the gas phase and the atomic structure of the interfaces, so we use it only as a guideline for choosing ϵ_{sf} . Interactions were truncated at $r_c = 2.5\sigma$, which is a common measure taken to accelerate simulations by reducing the number of interactions that must be computed. The surface tension γ is the only parameter we use that is significantly sensitive to this procedure. For the temperature of our flow, $T = 1.0\epsilon/k_B$, γ is about a factor of two less than its $r_c \rightarrow \infty$ value⁹ but well defined nonetheless. The observed equilibrium liquid–vapor density ratio is $\rho_l/\rho_v = 12.1$. The triply periodic simulation domain had dimensions $L_x \times L_y \times L_z = 77.78r_o \times 52.33r_o \times 5.66r_o$. For clarity we normalize dimensions by $r_o = 2^{1/6}\sigma$ which is the zero-force radius and thus a good definition of the atomic diameter. Previous atomistic simulations of moving contact lines^{10–12} have illuminated some of the mechanics, but have not provided flow statistics in both the liquid and displaced vapor for a steadily advancing contact line, so they have not been able to investigate the possible role of flow driven phase change.

Newton's equation of motion was integrated numerically using the popular velocity Verlet algorithm with a time step of $\Delta t = 0.0046\sqrt{m\sigma^2/\epsilon}$. Flow was induced by a constant force acting on every fluid atom in the negative x direction. Net momentum was conserved by applying an equal and opposite net force to the wall atoms. Viscous heating was countered by periodically rescaling the atomic velocities, which, of course, violates the strict statistical mechanical formalism of the ensemble, but in practice the results we report

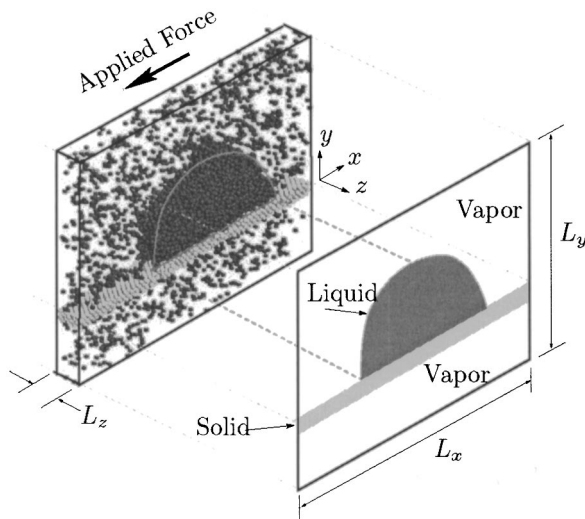


FIG. 1. Flow schematic. Periodic boundary conditions are used to model an infinite two-dimensional roll of fluid.

are utterly insensitive to this rescaling because the viscous heating was so slow.

Statistical quantities were computed in an array of 100×100 data bins in x and y in a frame fixed in x to the drop's center of mass and in y to the wall's center of mass. Each time step, mean values of flow quantities in each bin were accumulated for time averaging. For the results presented here, statistics were accumulated in several ensembles over a net simulation time of $9 \times 10^6 \sqrt{m\sigma^2/\varepsilon}$. Such a long simulation was necessary to converge velocity statistics since atomic velocities were $\sim 10^3$ times higher than mean flow velocities.

We report two cases in this Letter. One has a driving force three times stronger than in the other, but they are otherwise identical. Relevant parameters are listed in Table I. We are in a low-Weber-number and low-capillary-number regime. The Peclet number is near unity and we will indeed see a qualitative change in behavior for the $Pe = 1.22$ versus the $Pe = 3.67$ case. Except when noted, results are for the $Pe = 3.67$ case. The Bond number is less than unity so we expect minimal deformation of the drop by the applied body force.

Figure 2 shows mean density contours. Most of the density change from liquid to vapor occurs over about $6r_o$, which would be 20 \AA for liquid argon. There is reasonable agreement with our anticipated contact angle of $\theta = 83^\circ$ and near symmetry at wetting and de-wetting. Advancing and

TABLE I. Flow parameters: external force applied to each fluid atom f , capillary number $Ca = \mu U/\gamma$, Weber number $Wb = \rho U^2 H/\gamma$, Peclet number $Pe = UH/D$, and Bond number $Bo = \rho a_b H^2/\gamma$, where U is the speed of the liquid-vapor interface relative to the wall, H is the $\rho = 0.5(\rho_v + \rho_l)$ height of the droplet, a_b is the applied acceleration that drives the flow, D is the auto-diffusivity of this Lennard-Jones liquid, and μ is the liquid's viscosity. Lennard-Jones μ , γ and D are assumed to be as reported for bulk (Refs. 9 and 15).

$f [\varepsilon/\sigma \times 10^{-5}]$	Ca	Wb	Pe	Bo
17.1	0.023	0.0012	1.22	0.066
5.7	0.072	0.012	3.76	0.200

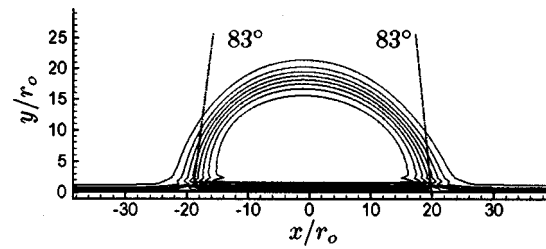


FIG. 2. Contours of density: eight evenly spaced contours between $0.1(\rho_l - \rho_v) + \rho_v$ and $0.9(\rho_l - \rho_v) + \rho_v$. The straight lines are drawn at exactly the anticipated contact angle of 83° . $y = 0$ is the mean position of the top wall atoms. The jagged contours near the wall are due to wall induced ordering of the fluid (Ref. 10).

receding contact angles differ by less than 10° . Little asymmetry is expected since the Bond number is small and the surface is obviously free of roughness, chemical inhomogeneities, or deposited solutes all of which which are thought to augment contact line hysteresis.⁸

Figure 3(a) shows streamlines for the high-force case. We see a flow similar to that observed macroscopically.¹ There is a clear rolling motion in the drop. There is a dividing streamline that originates at the wetting common line and extends into the vapor being displaced by the liquid, but we also see an evaporation of fluid through the advancing interface in close qualitative agreement with phase-field models.⁵⁻⁷ At the wetting common line in Fig. 3(b), the streamlines in fluid with less than approximately half the mean liquid-vapor density exit above the advancing common line. Thus, the fluid velocity is different than the interface velocity, which like slip can relieve the stress singularity.^{5,6}

At de-wetting, however, we see a different behavior [Fig. 3(c)]. Macroscopic observations show that a dividing streamline originates in the vapor phase and terminates at the receding contact line. However, we observe no such injection of fluid toward the de-wetting common line. Instead, there is an evaporative flow of fluid out of the droplet from the receding contact line, which would counteract the injection of fluid toward this point. The entire domain of this simulation is much smaller than what can be observed in an experiment, so it is not surprising that such an evaporative flux has not been observed. If this simulation were of a larger drop, we anticipate that this evaporative ejection would meet an injection further away from the contact line.

Linearized phase-field models predict wetting and de-wetting to be symmetric, but simulations incorporating non-linearity are reported to show asymmetric behavior.⁵ For de-wetting $Ca > 0.008$ de-wetting contact line fails and switches to a film formation behavior. Here we see a strong evaporative flux out of the de-wetting contact line, which could potentially form a wall film for some parameters. However, preliminary results still show substantial evaporation even for significantly greater fluid-solid affinity.

In the lower Pe case [Fig. 3(d)], the region with mass flux through the liquid-vapor interface becomes more extensive, as anticipated by phase-field models. In the Cahn-Hilliard-van der Waals diffuse mean-field framework the mobility κ , which is proportional to the diffusivity, sets the

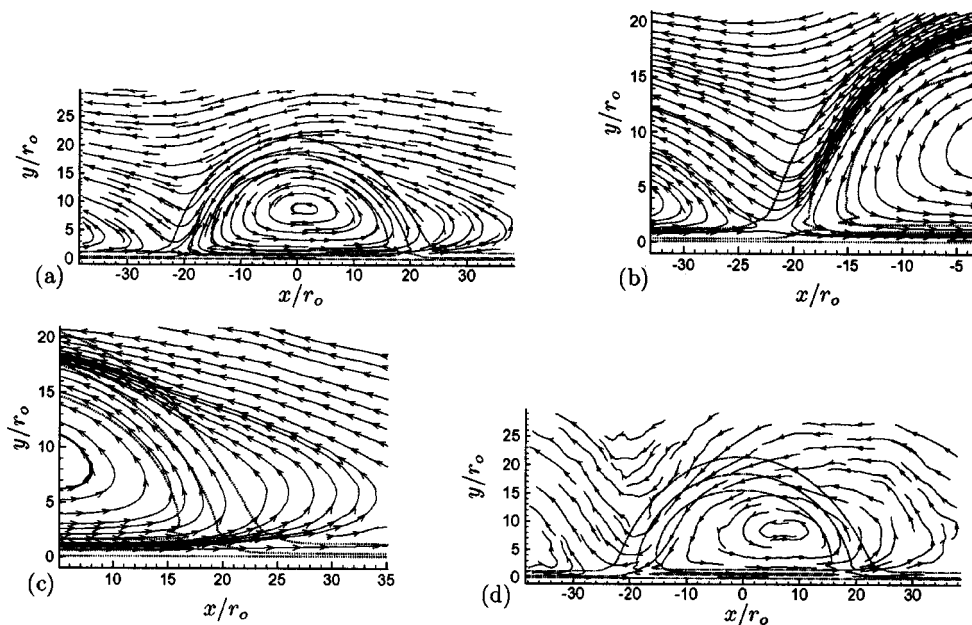


FIG. 3. Streamlines: (a) high-force case; (b) close-up of wetting in high-force case; (c) close-up of de-wetting in high-force case; and (d) low-force case. Dotted lines show the 10, 50, and 90 percent density contours.

scale ($\sim \kappa^{1/2}$) and intensity ($\sim \kappa^{-1/2}$) of the chemical potential that drives a phase changing mass flux through the interface.⁵ Thus we anticipate a change in the transport of the droplet along the surface as we tip the balance between diffusive and convective fluxes as parametrized by Pe , the higher Pe case being, of course, more directly relevant to the macroscopic case.

Evaporation and condensation are more precisely quantified by the material derivative of the density,

$$\frac{D\rho}{Dt} = -\rho \nabla \cdot \mathbf{u}, \tag{1}$$

which will be negative where there is a net evaporative flux and positive where there is a net condensation flux. The contours in Fig. 4 show that there is indeed substantial net evaporation near the receding contact line and there is evaporation above the advancing contact line. $D_t \rho$ is positive at the advancing contact line where the wall film is absorbed into the droplet as shown by the streamlines in the first r_o above the wall in Fig. 3(b). For our ε_{sf} , this layer is made of scattered fluid atoms that sit on the wall and assume nearly the wall velocity. They enter the droplet at the advancing

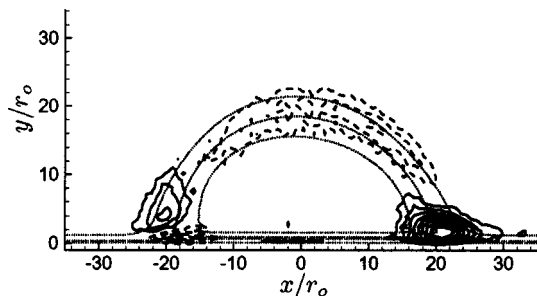


FIG. 4. $D_t \rho = -\rho \nabla \cdot \mathbf{u}$, showing regions of significant expansion (evaporation) and compression (condensation). Contours are evenly spaced levels with increment $5.7 \times 10^{-5} \sqrt{\varepsilon m} / \sigma^4$. Positive contours are dashed. The zero contour is omitted. The data were smoothed before plotting.

contact line, but their residence time is short and they do not seem to be dynamically significant. Away from the contact lines on the top of the drop, there is a distributed net condensation, which preserves the overall mass balance. The thermodynamics of the phase change have not yet been investigated.

Slip near the contact line is a convenient boundary condition for continuum models, but slip has only been observed directly in atomistic simulations of immiscible fluids.^{10,12} Figure 5(a) shows the region where the wall strain rate is high in advance of the wetting common line. This is where phase-field models also suggest that there would be the highest strain rate and possibly slip. Figure 5(b) shows velocity profiles. We see that there is a relatively large jump close to the wall suggestive of a slip velocity ahead of the drop. The

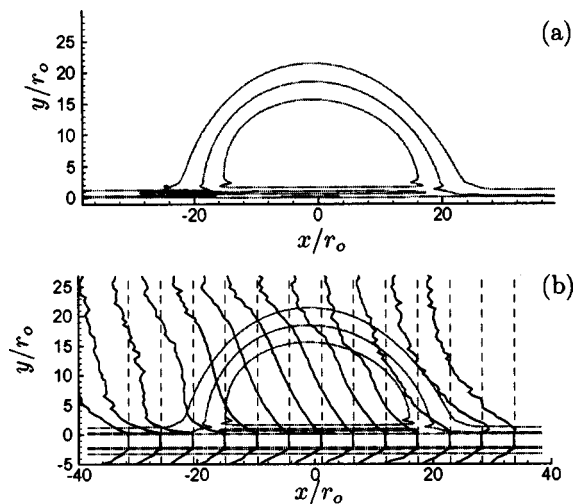


FIG. 5. (a) Contours showing region of high (negative) shear stress: three contours from $-0.006 \sqrt{\varepsilon / \sigma^2 m}$ to $-0.010 \sqrt{\varepsilon / \sigma^2 m}$, which is close to the maximum (negative) wall shear. The positive peak was only $0.002 \sqrt{\varepsilon / \sigma^2 m}$ at $x = 27.2 r_o$, which is just behind the de-wetting contact line. (b) Velocity profiles suggesting slip in advance of wetting contact line.

maximum observed u_s across a single atomic thickness is $u_s \approx 0.009\sqrt{\varepsilon/m}$. The slip length¹³ defined by $u_s/\lambda = \partial_y u$ is estimated to be $\lambda \approx 2\sigma$, but precision is not possible due to the coarseness of bins used to accumulate statistics. Just behind the de-wetting contact line there is a monolayer of fluid atoms that are actually moving slightly faster than the wall, which might also be interpreted as a slip, though of lesser degree than before the drop.

So, we have shown that for this case of a liquid drop in equilibrium with its own vapor that evaporation and condensation are substantial components of the flow and at wetting appear to act as anticipated in phase-field models of moving contact line flows.^{5,7} The evaporative flux above the advancing contact line will in part relieve the stress singularity at the wetting contact line, though we also observe some slip in the gas phase. We do not observe as significant a slip at the de-wetting contact line. Instead, there is a substantial evaporative flux at this common line. Closer comparison with phase-field model predictions is warranted.

The drop we have considered is obviously many times smaller than can be studied in experiment. However, we anticipate that for drops of more realistic sizes there will be a region of scale ℓ such that $Pe_\ell \approx 1$ where the phenomena that we observe are significant, as least for miscible fluids. Previous work using atomistic simulations^{10,12} in the immiscible limit suggest that there is only a small region of slip that relieves the stress singularity. Here we find both slip and evaporative flux. A further examination of cases between the present highly soluble system and immiscible systems is necessary before firm statements about the general mechanism can be made. We anticipate slip models for immiscible fluids, such as the recent proposal of Cox,³ to be more applicable in this limit.

Future work on less miscible fluids should also consider the recent surface tension relaxation model of Shikhmurzaev,¹⁴ which was designed for this case. In the present simulations, we have computed the mean force on

the atoms in the diffuse layers, which is a measure of the local surface tension and can thus show how it changes near the wall. We find that like the geometry this force is nearly symmetric for wetting versus de-wetting. It also only varies slowly like the curvature to within $\sim 1.5r_o$ of the wall, so if there is significant surface tension relaxation, it occurs within an atomic diameter or so of the wall atoms. This is less than the thickness of the diffuse interface.

¹E. B. Dussan V. and S. H. Davis, "On the motion of a fluid-fluid interface along a solid surface," *J. Fluid Mech.* **65**, 71 (1974).

²L. M. Hocking, "A moving fluid interface. Part 2. The removal of the force singularity by a slip flow," *J. Fluid Mech.* **79**, 209 (1977).

³R. G. Cox, "Inertial and viscous effects on dynamic contact angles," *J. Fluid Mech.* **357**, 249 (1998).

⁴R. Goodwin and G. M. Homsy, "Viscous flow down a slope in the vicinity of a contact line," *Phys. Fluids A* **3**, 515 (1991).

⁵D. Jacqmin, "Contact-line dynamics of a diffuse fluid interface," *J. Fluid Mech.* **402**, 57 (2000).

⁶L. M. Pismen and Y. Pomeau, "Disjoining potential and spreading of thin liquid layers in the diffuse-interface model coupled to hydrodynamics," *Phys. Rev. E* **62**, 2480 (2000).

⁷P. Seppelcher, "Moving contact lines in the Cahn-Hilliard theory," *Int. J. Eng. Sci.* **34**, 977 (1996).

⁸P. G. de Gennes, "Wetting: Statics and dynamics," *Rev. Mod. Phys.* **57**, 827 (1985).

⁹M. Mecke, J. Winkelmann, and J. Fischer, "Molecular dynamics simulation of the liquid-vapor interface: The Lennard-Jones fluid," *J. Chem. Phys.* **107**, 9264 (1997).

¹⁰J. Koplik, J. R. Banavar, and J. F. Willemsen, "Molecular dynamics of fluid flow at solid surfaces," *Phys. Fluids A* **1**, 781 (1989).

¹¹M. J. de Ruijter, T. D. Blake, and J. De Coninck, "Dynamic wetting studied by molecular modeling simulations of droplet spreading," *Langmuir* **15**, 7836 (1999).

¹²P. A. Thompson and M. O. Robbins, "Contact-line motion: Slip and the dynamic contact angle," *Phys. Rev. Lett.* **63**, 766 (1989).

¹³C. L. M. H. Navier, *Memoirs de l'Academie Royale des Sciences de l'Institut de France* **1**, 414 (1823).

¹⁴Y. D. Shikhmurzaev, "Moving contact lines in liquid/liquid/solid systems," *J. Fluid Mech.* **334**, 211 (1997).

¹⁵K. Meier, A. Laesecke, and S. Kabelac, "A molecular dynamics simulation study of the self-diffusion coefficient and viscosity of the Lennard-Jones fluid," *Int. J. Thermophys.* **22**, 161 (2001).